



# CO<sub>2</sub>-responsive aqueous foams stabilized by pseudogemini surfactants

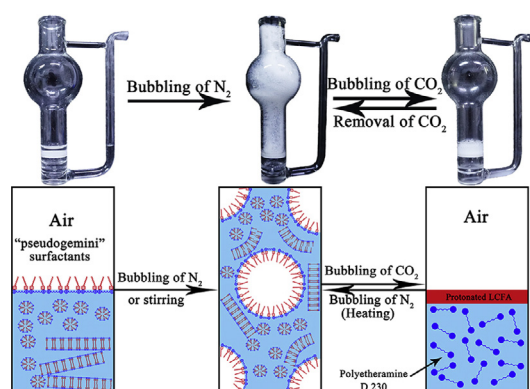
Zengzi Wang<sup>a</sup>, Gaihan Ren<sup>a</sup>, Jiawen Yang<sup>a</sup>, Zhenghe Xu<sup>b,c</sup>, Dejun Sun<sup>a,\*</sup>

<sup>a</sup> Key Laboratory of Colloid and Interface Chemistry, Shandong University, Ministry of Education, Jinan, Shandong 250100, PR China

<sup>b</sup> Department of Materials Science and Engineering, Southern University of Science and Technology, Shenzhen, Guangdong 518055, PR China

<sup>c</sup> Department of Chemical and Materials Engineering, University of Alberta, Edmonton, Alberta T6G 1H9, Canada

## GRAPHICAL ABSTRACT



## ARTICLE INFO

### Article history:

Received 19 September 2018

Revised 13 October 2018

Accepted 15 October 2018

Available online 16 October 2018

### Keywords:

Pseudogemini surfactants

Long chain fatty acids

Polyetheramine

CO<sub>2</sub> responsive foam

## ABSTRACT

**Hypothesis:** To obtain surfactants with superior surface activity and responsive behavior, “pseudogemini” surfactants (short for D-LCFA) are synthesized by mixing long chain fatty acids (LCFA) and polyetheramine D 230 at fixed molar ratio (2:1). Non-covalently bonded building blocks indicate that CO<sub>2</sub>-responsive aqueous foams can be obtained by utilizing such pseudogemini surfactants.

**Experiments:** <sup>1</sup>H NMR and FT-IR characterizations prove that the building blocks of these surfactants are associated by electrostatic interaction. The synthesis (Brønsted acid-base reaction) is simple and eco-friendly. “Pseudogemini” structure enables D-LCFA to reduce surface tension of aqueous solution effectively, thus facilitating foam generation. Rheograms, FF-TEM and Cryo-TEM results prove that different aggregates in D-LCFA aqueous solutions lead to different foam properties.

**Findings:** Bubbling of CO<sub>2</sub> for about 30 s leads to the rupture of aqueous foams generated by D-LCFA, while removing CO<sub>2</sub> by bubbling of N<sub>2</sub> at 65 °C for 10 min enables re-generation of foams. The CO<sub>2</sub>-responsive foaming properties can be attributed to dissociation of D-LCFA upon bubbling of CO<sub>2</sub> and re-association upon removal of CO<sub>2</sub>. The effective CO<sub>2</sub>-responsive foams can be applied to many areas, such as foam fracturing, foam enhanced oil recovery or recovering of radioactive materials.

© 2018 Elsevier Inc. All rights reserved.

## 1. Introduction

Foams are dispersions of gas in liquid or solid matrices, which have small diameters, high surface area and excellent flow characteristics [1]. They have been widely used in many areas, such as

\* Corresponding author.

E-mail address: [djsun@sdu.edu.cn](mailto:djsun@sdu.edu.cn) (D. Sun).

food, firefighting, oil recovery, mineral flotation and preparation of porous materials [2–4]. In many situations foams only need to be stabilized temporarily to avoid the contamination or difficulties in processing of excess foams. However, during the defoaming process, high cost and contamination brought by defoamers can be troublesome. To destabilize foams effectively and avoid the disadvantages of defoamers, utilizing responsive foaming agents will be a green alternative [5,6]. The stability of foams generated by responsive foaming agents can be controlled by external triggers including pH [7–9], temperature [10–12], light [13–15], magnetic field [16] and/or CO<sub>2</sub> [17–19]. Compared with other triggers with several limitations, CO<sub>2</sub> can be regarded as a non-toxic, inexpensive and readily removable trigger [20]. Jessop et al. [18] reported switchable long chain alkyl amidine as CO<sub>2</sub>-responsive surfactant. In the presence of CO<sub>2</sub> and water, long chain alkyl amidine is protonated into charged amidinium bicarbonate, which has excellent surface activities. Removing CO<sub>2</sub> by inert gas (Ar) at 65 °C converts the protonated amidinium bicarbonate back to neutral alkyl amidine of little surface activity.

However, alkyl amidines are usually of high cost and need complicated synthesis. As supramolecular amphiphiles have been widely applied [21], new CO<sub>2</sub>-responsive surfactants based on non-covalent interaction could be synthesized inexpensively and conveniently. For example, neutralizing LCFA (long chain fatty acid) by amine is a good choice to prepare CO<sub>2</sub>-responsive surfactants (short for amine-LCFA). The amine and LCFA are associated by electrostatic interaction, which can be regarded as typical non-covalent bond. “Pseudogemini surfactants” are a series of surfactants with similar structure as gemini surfactants. Their hydrophilic spacers and hydrophobic tails are also associated by non-covalent bond. “Amine-LCFA” type pseudogemini surfactants are fascinating for their compact adsorption at interface, high surface activity and easier preparation. Many researchers fabricated interesting aggregates based on such pseudogemini surfactants. For example, Li et al. [22] applied sebacic acid and C<sub>14</sub>DMAO at molar ratio of 1:2 to prepare a novel pseudogemini surfactant (C<sub>14</sub>-S-C<sub>14</sub>). Polymorphic aggregation of pseudogemini surfactant was observed in the C<sub>14</sub>-S-C<sub>14</sub>/H<sub>2</sub>O system. A variety of bilayers including unilamellar vesicles, onions, and hyper branched bilayers were formed in the system. Zheng et al. [23] designed pseudogemini surfactants utilizing anionic surfactant SDBS and small molecule cationic spacers ([mim-C<sub>4</sub>-mim] Br<sub>2</sub> and [mpy-C<sub>4</sub>-mpy] Br<sub>2</sub>) at a molar ratio of 2:1. Vesicles were generated by these surfactants. The relationship between vesicle formation and weak interaction was also investigated. Feng et al. [17] reported one kind of CO<sub>2</sub>-responsive wormlike micelles fabricated by pseudogemini surfactant (SDS-TMPDA). These wormlike micelles have excellent viscoelastic properties, and can be tuned by bubbling/removing of CO<sub>2</sub>.

However, using conventional amines as building blocks of pseudogemini surfactant lead to high biological toxicity [24], which severely limited their applications. Introducing ethylene oxide (EO) or propylene oxide (PO) groups to the backbone can significantly reduce the toxicity of amines [25,26]. These so-called “polyetheramines” have advantages of low molecular weight, high water solubility and reduced biological toxicity [27,28]. Low-toxic and hydrophilic polyetheramines can be served as spacers. For example, polyetheramine ED 900, which possess two primary amine group, was applied to prepare pseudogemini surfactants by simply mixing with LCFA at molar ratio of 1:2 [25]. Thorough investigations on their phase behavior were carried out, and these ED 900-LCFA micelles were used as templates for synthesis of SiO<sub>2</sub> mesoporous materials [26].

In spite of thorough investigation into aggregates formed by pseudogemini surfactants, few attention was paid to their responsive behavior brought by electrostatic interaction, let alone respon-

sive emulsions or foams stabilized by pseudogemini surfactants. In our previous work, polyetheramine D 230 and oleic acid (HOA) were used to prepare pseudogemini surfactant “D-OA” of CO<sub>2</sub>-responsive interface activity [29,30]. The D-OA was used to prepare CO<sub>2</sub>-responsive emulsions, which has been applied to enhancing oil recovery. In this paper, considering the similarity between emulsions and foams, it is hypothesized to obtain CO<sub>2</sub>-responsive aqueous foams by utilizing similar pseudogemini surfactants.

To obtain aqueous foams with different properties, we prepared a series of pseudogemini surfactants by simply mixing polyetheramine D 230 and LCFA (lauric acid, myristic acid, palmitic acid and stearic acid, short for C12, C14, C16 and C18, respectively). The surfactants are named as D-LCFA (D-C12, D-C14, D-C16 and D-C18, respectively). D-LCFA aqueous solutions were shown to generate foams with different properties, which can be explained by the aggregate properties in solution. Bubbling of CO<sub>2</sub> into aqueous foams generated by D-LCFA solutions led to rapid collapse of the foams, while bubbling of N<sub>2</sub> at 65 °C enabled the re-generation of aqueous foams. These CO<sub>2</sub>-responsive aqueous foams may have potential applications in situations where rapid defoaming/re-foaming on demand is required [5].

## 2. Experimental section

### 2.1. Materials

Polyetheramine D 230 of molecular weight  $\approx$  230 was purchased from Sigma-Aldrich (also named as Jeffamine D 230, technical grade), which is a primary diamine with the poly (oxypropylene) ( $n \approx 2-3$ ) as its backbone. LCFA (lauric acid (C12), myristic acid (C14), palmitic acid (C16), stearic acid (C18), all AR), salts (NaCl and CaCl<sub>2</sub>, all AR) and sodium carboxylates (sodium laurate and sodium stearate, all AR) were obtained from Sinopharm Chemical Reagent Co. Ltd., China. All the reagents (Scheme 1a) were used as received. Deionized water was used in all the experiments.

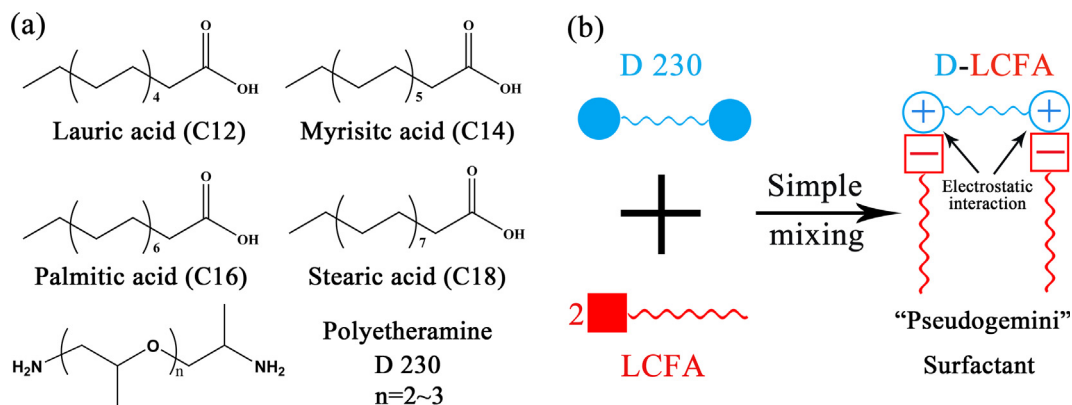
### 2.2. Synthesis of pseudogemini surfactant D-LCFA

D-LCFA was synthesized through Brønsted acid-base reaction, i.e., simple mixing of long chain fatty acids with D 230 at a molar ratio of 2:1. The LCFA was heated and maintained at 75 °C under nitrogen atmosphere to melt LCFA. D 230 was then added dropwise into the liquid LCFA, and the mixture was stirred at 400 rpm for 30 min. After which, D-LCFA was dried under vacuum for 6 h. Electrostatic interaction between two building blocks enables the formation of pseudogemini surfactant, as shown in Scheme 1b. The structure of D-LCFA was characterized by FT-IR (NEXUS 670, Thermo Nicolet) and <sup>1</sup>H NMR (Bruker Avance 400 spectrometer, 400 Hz, CDCl<sub>3</sub>).

### 2.3. Surface tension measurement

#### 2.3.1. Static surface tension

The surface tension and critical micelle concentration (CMC) of different D-LCFA aqueous solutions were measured by a Sigma 700 (Biolin/Attension) force tensiometer using the plate method. The temperature was controlled at 25 °C with a water bath. The glass cell was cleaned with ethanol and rinsed with water repeatedly. The platinum plate was flamed to burn off any organic contaminants prior to its use. To obtain curves of surface tension vs different concentration, original D-LCFA aqueous solutions (10 mM) were injected into deionized water under programmed scheme. Each test was repeated at least in triplicate until the difference between the measurements was negligible.



**Scheme 1.** (a) Structures of long chain fatty acids and D 230. (b) Preparation of D-LCFA by simple mixing of LCFA with D 230.

### 2.3.2. Dynamic surface tension

Dynamic surface tension of D-LCFA aqueous solutions and air was measured using a Drop Profile Analysis Tentiometer (Tracker, France). Images were captured during the formation of an air droplet (3  $\mu\text{l}$ ) in 0.05 mM D-LCFA aqueous solution. The surface tension was calculated using Laplace equation from the curvature of the droplet obtained by analyzing the images captured.

### 2.4. Foam properties (foamability and foam stability) measurement

Four methods of generating foams were applied in our work.

#### 2.4.1. Handshaking

Aqueous foams were generated in glass flask (20 ml) by vigorously shaking of 10 ml D-LCFA aqueous solutions.

#### 2.4.2. Waring blender stirring

In order to obtain more accurate data of foam properties, the D-LCFA aqueous solutions (150 ml, 20 mM) were stirred by waring blender at 5000 rpm for 60 s. Then foams were then transferred into the graduated glass cylinder and stored at ambient temperature. Foamability was determined by the foam volume. Foam stability was measured by observing the foam height as a function of time.

#### 2.4.3. Foamscan

To obtain the accurate value of half-life time of foams, an HT FOAMSCAN apparatus (TECLIS, France) was used to measure the foam properties. The change of the bubble state in the foam was observed by a CCD (Charge-coupled Device) camera, which photographed every 2 s after  $\text{N}_2/\text{CO}_2$  flow stopped. The pictures were analyzed with CSA (Cell Size Analysis) software, which generated the results of bubble size and size distribution. In this case, 60 ml solution was first injected into the glass tube. The foams were generated by blowing  $\text{N}_2$  through a porous glass filter at the required flow rate of 200 ml/min. The variation of the liquid content of the foam was measured by five pairs of electrodes located along the glass column, labeled as the first, the second, the third, the fourth, and the fifth pair of electrode from the bottom to the top. All of the electrodes were made from stainless steel materials. Except for measuring the liquid content of the foam, electrodes were also used to record the foam volume in real time. In all the experiments, the input of  $\text{N}_2/\text{CO}_2$  was stopped when the foam volume reached 200 ml, and the evolution of foam was analyzed.

#### 2.4.4. Bubbling device

To get a better image of  $\text{CO}_2$  responsive foaming and defoaming in graphic abstract, a bubbling device (Scheme S1) provided by Cui

et al. [31] was applied in this work. 5 ml D-LCFA aqueous solutions (20 mM) were added into the device and gas was injected at 400 ml/min to generate or destabilize foams.

### 2.5. Aggregates characterization

Several methods were applied to characterizing the aggregates in different D-LCFA aqueous solutions.

#### 2.5.1. Rheograms

The apparent shear viscosity of D-LCFA solutions was measured using a standard Haake Rotational Rheometer (Haake RS 75) with a concentric cylinder geometry system Z41-Ti. The thickness of the sample in the middle of the sensor was 3.0 mm. The test samples (D-LCFA 12 ml, 20 mM) were sheared at a programmed  $\gamma$  (shear rate) increasing from 0.1 to 1000  $\text{s}^{-1}$  in 5 min to obtain flow curves, and the steady-shear viscosity versus the shear rate was obtained. During the measurements, the temperature was held constant at 25  $^\circ\text{C}$  by a water circulating thermal bath.

#### 2.5.2. Freeze-Fracture transmission electron microscope (FF-TEM)

The microstructure of the bilayers was characterized by FF-TEM observations. A trace amount of solution was placed on a 0.1 mm-thick copper disk and covered with a second copper disk. The sample sandwiched between the copper disks was frozen rapidly by plunging the sandwich into a liquid propane cooled by liquid nitrogen. Fracturing and replication of the foams were carried out at about  $-140\text{ }^\circ\text{C}$ . Pt/C was deposited at an angle of  $45^\circ$  on the fractured samples. The prepared sample was examined in a JEM-1011 electron microscope (JEOL Ltd.) operated at 80 kV.

#### 2.5.3. Cryogenic transmission electron microscopy (Cryo-TEM)

Within a high-humidity environment ( $>90\%$ ), the sample was dropped on a grid. The excess sample was blotted up with two pieces of blotting paper, leaving a thin film sprawling on the grid. The grid was then plunged into a liquid ethane which was then frozen by liquid nitrogen. The vitrified sample was transferred to a sample holder (Gatan 626) and observed on a JEOL JEM-1400 TEM (120 kV) at about  $-174\text{ }^\circ\text{C}$ . The images were recorded on a Gatan multiscan CCD.

#### 2.5.4. Aggregate size measurement

The size of the aggregates in D-LCFA aqueous solutions was measured at 25  $^\circ\text{C}$  on a Malvern particle size analyzer (ZetaPALS, Brookhaven, USA). 20 mM D-C12 and D-C14 aqueous solutions were measured. Each measurement was performed in triplicate.

## 2.6. pH and conductivity measurements

In order to confirm the reversibility and repeatability of solution switching, pH (PB-10 pH meter, Sartorius, Germany) and conductivity (Leici conductivity meter, Pt/platinized electrode with a cell constant of  $1.02 \text{ cm}^{-1}$ ) of D-LCFA aqueous solutions were measured under alternate bubbling and removal of  $\text{CO}_2$ .

## 3. Results and discussion

### 3.1. Structure characterization of D-LCFA

The chemical structure of “pseudogemini” surfactant D-LCFA (Scheme 1b) was characterized by FT-IR and  $^1\text{H}$  NMR. The FT-IR spectra of C18 (stearic acid), D 230 and D-C18 are shown in Fig. 1. On the spectrum of C18, only one carbonyl peak at  $1710 \text{ cm}^{-1}$  was observed and no carboxylate peaks were seen ( $1562 \text{ cm}^{-1}$  for fully neutralized C18), which indicates the absence of dissociated  $-\text{COOH}$  groups. This result can be explained by the dimeric form of fatty acids. One fatty acid molecule bonded to another by hydrogen bond, and thus no more dissociated  $-\text{COOH}$  group existed [32]. After neutralized by D 230, the carbonyl peak at  $1710 \text{ cm}^{-1}$  of C18 moved to 1562 and  $1401 \text{ cm}^{-1}$ , indicating the conversion of  $-\text{COOH}$  to  $-\text{COO}^-$ . The peaks at  $3372 \text{ cm}^{-1}$  and  $3295 \text{ cm}^{-1}$  in the high wavenumber region of D 230 spectrum corresponded to asymmetric and symmetric stretching vibrations of  $-\text{NH}_2$ , respectively, with the bending vibrations of  $-\text{NH}_2$  at  $1589 \text{ cm}^{-1}$ . Similarly, no stretching vibration band was observed at high wave numbers on the spectrum of D-C18, and the bending vibrational peak was moved from  $1589 \text{ cm}^{-1}$  to  $1636 \text{ cm}^{-1}$ . These results clearly indicate the formation of  $-\text{NH}_3^+$  and  $-\text{COO}^-$  via proton transfer from  $-\text{COOH}$  to  $-\text{NH}_2$ , proving the electrostatic interaction between D 230 and C18. For other D-LCFA (Fig. S1), similar shift of their characteristic peaks was observed.

$^1\text{H}$  NMR spectra of C18 and D-C18 in  $\text{CDCl}_3$  were shown in Fig. 2. The  $^1\text{H}$  chemical shifts of  $\alpha$  and  $\beta$   $-\text{CH}_2$  groups near  $\text{C}=\text{O}$  group in C18 moved upfield due to the increased electron density, indicating the transformation of  $-\text{COOH}$  to  $-\text{COO}^-$ , further confirming electrostatic interaction between D 230 and LCFA. Similar chemical shifts in  $^1\text{H}$  NMR spectra of other D-LCFA were also observed (Fig. S2). In addition, ionization of building blocks was also proved by conductivity vs temperature curves, which has been explained in Fig. S3 and Table S1 in detail.

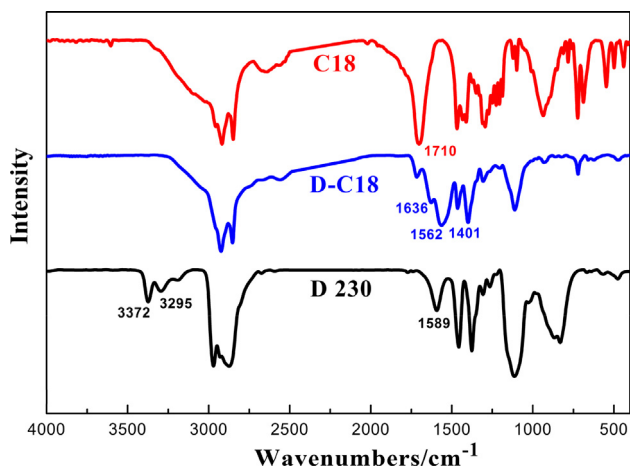


Fig. 1. FT-IR spectra of stearic acid (C18), polyetheramine D 230 and D-C18.

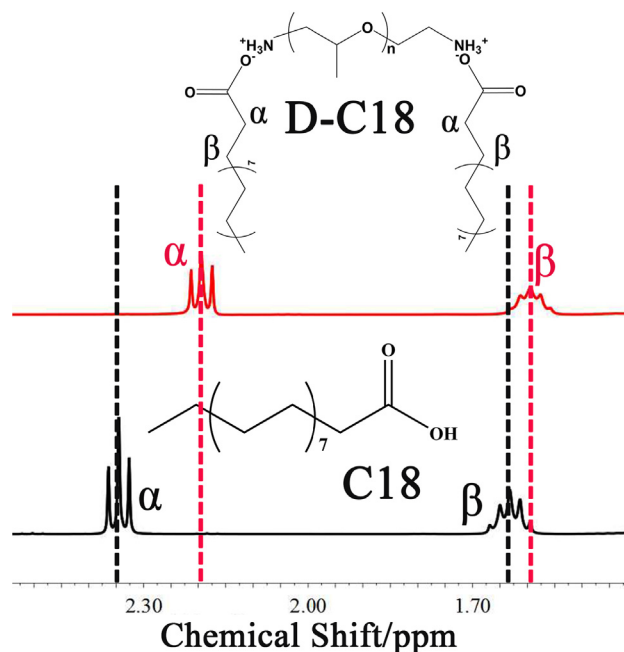


Fig. 2.  $^1\text{H}$  NMR spectra of C18 and D-C18.

### 3.2. Properties of aqueous foams stabilized by D-LCFA

#### 3.2.1. Surface tension and critical micelle concentration (CMC) of D-LCFA

As one kind of pseudogemini surfactant, D-LCFA has excellent ability of reducing surface tension. As shown in Fig. 3, with increasing concentration, surface tension of D-LCFA aqueous solutions was reduced to low values, illustrating high surface activity. The break point in the surface tension-concentration plot can be considered as CMC (critical micelle concentration). In this work, CMC was also determined by conductivity methods (Fig. S4). According to Table 1, no obvious difference was observed for CMC values of D-LCFA tested by two means, and their CMC values are much lower than those of conventional surfactants (single chain neutralized fatty acids). Low CMC of D-LCFA can be explained by its “Gemini-like” structure. Double hydrophobic chains in one molecule make it more disruptive than single chain surfactants, which leads to promoted migration to the interface [33] and superior sur-

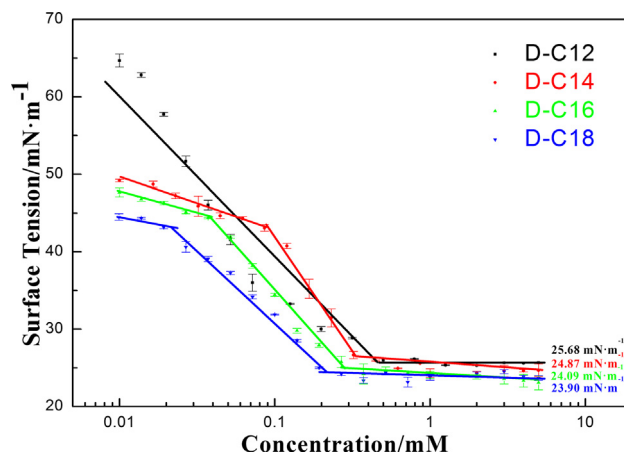


Fig. 3. Surface tension of D-LCFA aqueous solutions at  $25 \text{ }^\circ\text{C}$  as a function of surfactant concentration. The values in figure mean the average surface tension of D-LCFA concentration higher than CMC.

**Table 1**  
CMC values of pseudogemini surfactants D-LCFA and conventional single chain surfactants.

CMC/mM	C12	C14	C16	C18
D 230 (by surface tension)	0.49	0.33	0.26	0.19
D 230 (by conductivity)	0.75	0.3	0.25	0.2
Na <sup>+</sup>	24.4 [35]	6.9 [35]	2.1 [36]	1.8 [36]

**Table 2**  
Foam volume vs time (foams generated by D-LCFA aqueous solution 150 ml, 20 mM). Volumes of 0 h were regarded as foamability of D-LCFA solutions. Reduction rates of foam volume were determined as foam stability. 1 h etc. means standing times of foams. The origin images of foams are listed in Fig. S5.

Foam volume/ml	0 h	1 h	6 h	24 h	72 h	168 h
D-C12	800	600	290	0	0	0
D-C14	450	285	260	70	0	0
D-C16	330	330	325	300	140	40
D-C18	340	340	340	330	260	130

face activity than conventional surfactants [34]. In addition, CMC and surface tension ( $\gamma_{\text{cmc}}$ ) of some conventional gemini surfactants are listed in Table S1, to compare with those of D-LCFA.

### 3.2.2. Foamability and foam stability of D-LCFA

High surface activity of D-LCFA indicates that they can generate and stabilize aqueous foams. To confirm this hypothesis, D-LCFA aqueous solutions were stirred vigorously by waring blender at 5000 rpm and foams were generated (Fig. S5). Compared with conventional surfactants, D-LCFA aqueous solutions showed much higher foamability and foam stability (Fig. S6), which can be explained by high surface active “pseudogemini” structures of D-LCFA.

It is evident that the foamability and foam stability of aqueous solutions are chain length dependent (Table 2). For aqueous foams stabilized by D-C12 and D-C14, destabilization was clearly observed after standing of the foams for only 1 h, with complete foam collapse in less than 24 h. In contrast, the volume of aqueous foams stabilized by D-C16 and D-C18 was reduced a little after standing for more than 24 h, indicating the enhanced foam stability with increasing chain length of D-LCFA. Foamscan results (Fig. 4) also showed an increased foam stability with increasing chain length of D-LCFA. For aqueous foams stabilized by D-C12 and D-C14, the half-life time was 740 s and 2803 s, respectively,

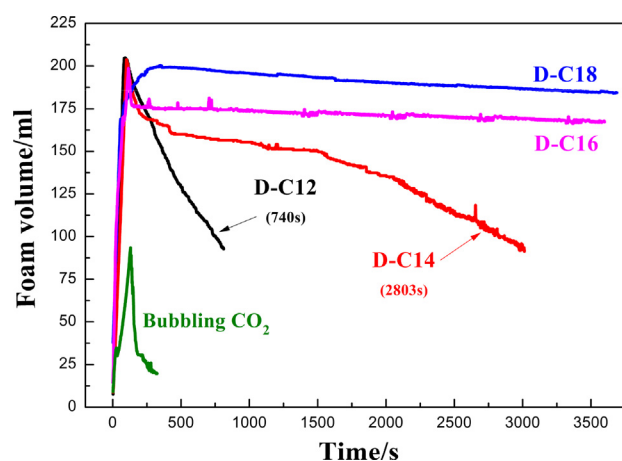


**Fig. 4.** Foam volume vs standing time of aqueous foams stabilized by D-LCFA solutions (60 ml, 20 mM). Green curve represented for replacing N<sub>2</sub> by CO<sub>2</sub> during foam generation. The half-life time of foams stabilized by D-C12 and D-C14 solutions was 740 s and 2803 s. The half-life time of foams stabilized by D-C16 and D-C18 cannot be detected within 3600 s.

in contrast to negligible change in foam volume after 1 h for the aqueous foams stabilized by D-C16 and D-C18.

With regard to foamability, D-C16 and D-C18 aqueous solutions possessed poorer foamability (330 ml and 340 ml, respectively), as compared to foamability of D-C12 and D-C14 aqueous solutions (800 ml and 450 ml, respectively). The relationship between foam properties and aggregates will be discussed later in this section.

### 3.2.3. Characterization of aggregates in D-LCFA solution

Aggregates in aqueous foams determine their foamability and foam stability [37,38]. The presence of bilayers near air-water interface will significantly improve the foam stability and reduce the foamability, while micelles cannot [6]. It is therefore necessary to determine the aggregates in D-LCFA aqueous solutions, both at macroscopic and microscopic levels.

To determine aggregates at a macroscopic level, solutions were observed under crossed polarizer, and rheograms were performed. Under crossed polarizer, the clear birefringence in D-C16 and D-C18 aqueous solutions (Fig. S7) indicated the existence of bilayers. In contrast, transparent and isotropic appearance of D-C12 and D-C14 aqueous solutions proved the presence of micelles rather than bilayers. Bilayers are known to significantly increase the viscosity of aqueous solutions, and they behave as two-dimensional liquids suspended in a three-dimensional solvent matrix, which makes bilayers sensitive to external forces [39,40]. D-C16 and D-C18 aqueous solutions possessed high viscosity and shear thinning properties (Fig. S8), indicating the possible existence of bilayers. However, more evidences should be provided by in-situ TEM observation, as similar properties can also be obtained by other aggregates. On the other hand, the viscosity of D-C12 and D-C14 solutions was very low and almost independent of shear rate, i.e. they are typical Newtonian fluid, which indicated the absence of certain aggregates (wormlike micelles, bilayers, etc.) in these solutions, according to similar conclusions obtained by Feng and Hao et al. [41,42].

To determine the aggregates at microscopic level, FF-TEM, Cryo-TEM and size measurements were utilized to obtain more direct evidence and quantitative data of aggregates. For D-C16 and D-C18 (Fig. S9) aqueous solutions, branched bilayers can be clearly seen by FF-TEM, while no obvious bilayer was seen in D-C12 and D-C14 solutions. Further details of bilayers were investigated by a Cryo-TEM. Clear images of branched bilayers of D-C16 and D-C18 (Fig. S10) aqueous solutions were obtained, with the interlayer spacing of 7.37 and 8.72 nm, respectively. In contrast, no bilayer including vesicles or lamellas was observed for D-C12 and D-C14 aqueous solutions. Only micelles were seen in these solutions (Fig. S11). The average size of aggregates for D-C12 and D-C14 aqueous solutions is 5.6 nm and 4.7 nm, respectively (Fig. S12).

According to Menger et al. [43], such aggregate size fall into the micellar range, thus further prove the existence of micelles.

### 3.2.4. Relationship between aggregates and foam properties

Packing parameter was often used to explain the morphology of self-assembled structure. The equation is given by  $p = v/af$ , where  $v$  is the volume of the hydrophobic chain,  $a$  is the optimal interfacial area per molecule, and  $f$  is the hydrophobic length normal to the interface. In most cases, the ratio  $v/af$  is a constant independent of tail length. Consequently, only the area  $a$  determine the value of  $p$  directly, which is influenced by the head group interactions [44]. Well-known connection between the  $p$  and the aggregate shape can be explained as: Sphere micelles for  $p \leq 1/3$ , cylinder micelles for  $1/3 \leq p \leq 1/2$ , bilayers for  $1/2 \leq p \leq 1$  and inverse micelles for  $p > 1$  [45,46]. Increasing chain length of hydrophobic tails led to stronger head group interaction (van der Waals interaction), thus decreasing value of  $a$  and increasing value of  $p$ , which can explain the formation of bilayers in D-C16 and D-C18 aqueous solutions.

For D-C16 and D-C18, high stability of aqueous foams generated by their aqueous solutions seems to be linked to compact, tight and ordered bilayers packed around bubbles. Bilayer surface layers have been proved to be capable of increasing apparent viscosity, slowing down gas diffusion process, and enhancing surface elastic modulus [37,38,47]. As a result, drainage flow, coalescence and coarsen will be inhibited, and foam stability will be significantly increased. For D-C12 and D-C14, poor stability of foams can be attributed to the absence of bilayers. According to the “smart foams” proposed by Fameau et al., only micelles in plateau border cannot reduce liquid film drainage rate and bubble coalescence effectively [6].

For D-C16 and D-C18, reduced foamability of their aqueous solutions can be explained by their slower adsorption, which is brought by both surfactant molecules and bilayers in solutions. For solution concentration below CMC (0.05 mM), dynamic surface tension curves (Fig. S13) of D-C16 and D-C18 need more time to achieve equilibrium state, indicating slower adsorption rate for D-C16 and D-C18 molecules. In addition, during foam generation, viscous bilayers in solutions need to be melted during foam generation and be re-formed after foam generation [37,48], thus slowing down adsorption rates. For D-C12 and D-C14, dynamic surface tension curves (Fig. S13) proved faster adsorption of their surfactant molecules. In addition, low apparent viscosity (without bilayer) leads to rapid adsorption dynamics and low adsorption energy barrier, resulting in enhanced foamability [49].

## 3.3. CO<sub>2</sub>-Responsive aqueous foam

### 3.3.1. CO<sub>2</sub>-responsive behavior of D-LCFA solutions

As a typical example of D-LCFA, D-C12 showed high solubility in the aqueous solution with pH of 8.34 (Fig. 5a, left). At this pH, LCFA was deprotonated (LCFA<sup>-</sup>) and D 230 was protonated (D 230<sup>2+</sup>). Bubbling of CO<sub>2</sub> (100 ml/min) into the solution for only 30 s made the transparent solution turbid (Fig. 5a, right). Increasing bubbling time to 120 s decreased the pH of turbid system to 6.02, accompanied with an increase in conductivity from 317 to 1174 μS/cm (Fig. 5b). During the CO<sub>2</sub> bubbling, newly formed H<sub>2</sub>CO<sub>3</sub> dissociated gradually to H<sup>+</sup> and HCO<sub>3</sub><sup>-</sup>. Increasing concentration of H<sup>+</sup> decreased solution pH to 6.02 at which the LCFA<sup>-</sup> became protonated completely. According to theories proposed by Kanicky et al. [50], decreasing pH of fatty acid soap system makes fatty acid droplets tend to accumulate at the surface, in the case of air/water system. In our system, with decreasing pH, protonated LCFA was insoluble in water as such that solution became turbid, indicating the disassociation of D-LCFA. Increasing concentration of H<sup>+</sup> and

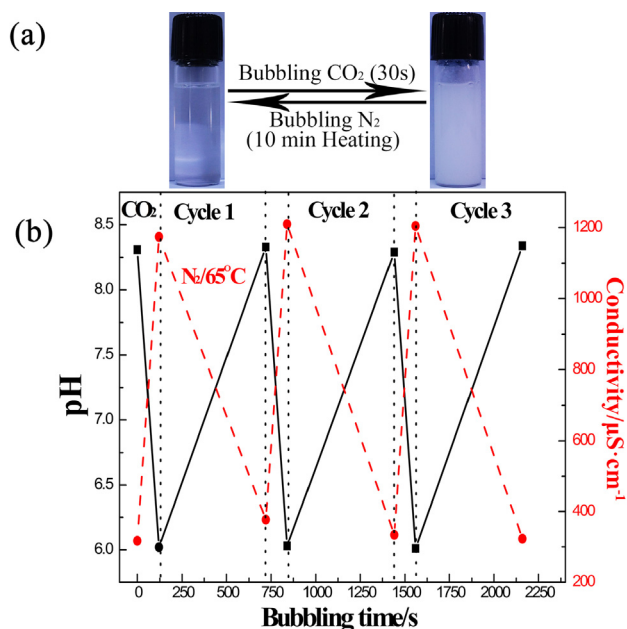


Fig. 5. (a) CO<sub>2</sub>-responsive behavior of D-C12 aqueous solutions (20 mM, 5 ml). (b) Changes in pH and conductivity under alternate bubbling of CO<sub>2</sub> and N<sub>2</sub> (65 °C).

HCO<sub>3</sub><sup>-</sup> in the system was proved by the increase in conductivity of solutions.

In order to re-form surface active D-LCFA, bubbling inert gas at high temperature (65 °C) to remove CO<sub>2</sub> is an effective way [18]. After bubbling of N<sub>2</sub> (100 ml/min) at 65 °C for 10 min, the turbid D-C12 system became transparent (Fig. 5a) with the pH and the conductivity returned to almost the same as their original value (Fig. 5b) of 8.31 and 377 μS/cm, respectively. The results indicated effective removal of CO<sub>2</sub>. Under the treatment of N<sub>2</sub> and heating, equilibrium shift of H<sub>2</sub>CO<sub>3</sub> by removal of CO<sub>2</sub> decreased the concentration of H<sup>+</sup> and HCO<sub>3</sub><sup>-</sup>. Deprotonation of LCFA and protonation of D 230 occurred with increasing pH. According to the results in Fig. 5b, pH and conductivity can be tuned by bubbling of CO<sub>2</sub>/N<sub>2</sub> for at least three cycles, which indicated the possibility of changing surface activity alternatively by bubbling of CO<sub>2</sub> and N<sub>2</sub> into the D-LCFA solution. For other D-LCFA with of different chain lengths, CO<sub>2</sub>-responsive properties were also observed (Fig. S14). In fact, CO<sub>2</sub>/N<sub>2</sub> responsive behavior in our work is caused by changing pH of D-LCFA solutions, and CO<sub>2</sub> and N<sub>2</sub> served as “pH regulators”, which is different from CO<sub>2</sub> responsive colloidal systems proposed by Jessop et al. [18,19,51], or CO<sub>2</sub> switchable aqueous foams proposed by Feng et al. [52,53]. However, it is not desirable to use conventional pH triggers here [54] (e.g., dilute HCl and NaOH solutions), as accumulating salts formed during alternative responsive process will significantly influence phase behavior of D-LCFA aqueous solutions (Fig. S15). In contrast, bubbling of CO<sub>2</sub>/N<sub>2</sub> will not bring any impurity into the system, which can be regarded as eco-friendly triggers.

### 3.3.2. CO<sub>2</sub>-responsive aqueous foams

CO<sub>2</sub>-responsive association and dissociation of D-LCFA indicate the possibility of generating CO<sub>2</sub>-responsive aqueous foams. As shown in Fig. 6, the volume of aqueous foams generated by D-C18 was reduced slightly after standing for 24 h. However, bubbling of CO<sub>2</sub> for only 30 s led to complete collapse of foams. Even after vigorous stirring for 1 min, no foam was generated, indicating complete defoaming by bubbling of CO<sub>2</sub>. According to the results in Fig. 4 from Foamscan, bubbling of CO<sub>2</sub> cannot generate foams effectively. Bubbling of N<sub>2</sub> at 65 °C for 10 min enabled the turbid

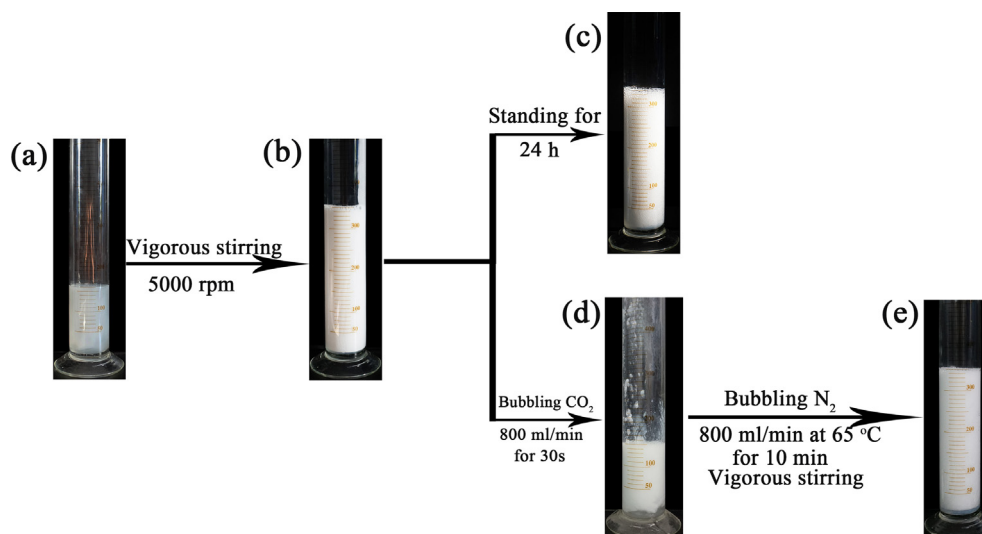


**Fig. 6.** (a) CO<sub>2</sub>-responsive process of foams generated by D-C18 aqueous solutions (150 ml 20 mM); (b) Stable foams obtained by stirring D-C18 solutions vigorously; (c) Very stable foams; (d) Bubbling of CO<sub>2</sub> led to the collapse of aqueous foams; and (e) bubbling of N<sub>2</sub> to re-stabilizing the foam.

solution to stabilize foams again. The above results proved the CO<sub>2</sub>-responsive foaming/defoaming properties of D-C18 aqueous solutions. In addition, D-LCFA with different chain lengths can generate CO<sub>2</sub>-responsive aqueous foams of different stability as shown in Fig. S16. More interestingly, it is possible for D-LCFA solutions to foam and defoam for five cycles upon alternative bubbling of CO<sub>2</sub> and N<sub>2</sub>.

### 3.3.3. Mechanism and potential application for CO<sub>2</sub>-responsive foaming and defoaming

The mechanism of CO<sub>2</sub>-responsive foaming/defoaming in D-LCFA solutions was proposed as shown in Fig. 7. During the formation of aqueous foams, surface active D-LCFA molecules adsorb at the air/water interface. More importantly, micelles (for all D-LCFA) or bilayers (for D-C16 and D-C18) are jammed in plateau borders to stabilize foams. Bubbling of CO<sub>2</sub> leads to disassociation of D-LCFA molecules and disassembly of aggregates (micelles and bilayers), resulting in the rapid collapse of foams. Due to the absence of surface active agents, few foam will be generated again. Removal of CO<sub>2</sub> upon bubbling of N<sub>2</sub> at high temperature enables the re-formation of D-LCFA molecules and corresponding aggregates. The foams are readily formed and stabilized again.

These CO<sub>2</sub>-responsive aqueous foams may have potential applications in situations where rapid defoaming/re-foaming on demand is required. For example, aqueous foams generated by D-LCFA with suitable viscosity and stability may be applied to foam fracturing. After finishing the fracturing, excess foams can be made to collapse in situ upon bubbling of CO<sub>2</sub>, rather than using expensive defoaming agents. The aqueous solutions can be reused upon removal of CO<sub>2</sub>, which meets the idea of green chemistry well [55]. More interestingly, according to Fameau et al. [5], such responsive foam may also be applied in textile, petrochemical, washing, environmental cleanup, and material recovery processes.

## 4. Conclusions

Building blocks of “pseudogemini” surfactants are associated via electrostatic interactions. Although pseudogemini surfactants have been widely applied to assembling different aggregates [22,25,26,56] and preparing responsive colloidal systems [17], little was reported on preparation of responsive foams using such surfactants. In this work, a series of pseudogemini surfactants (D-LCFA), prepared by simple mixing of long chain fatty acids (LCFA) with polyetheramine (D 230) at molar ratio of 2:1, were proved

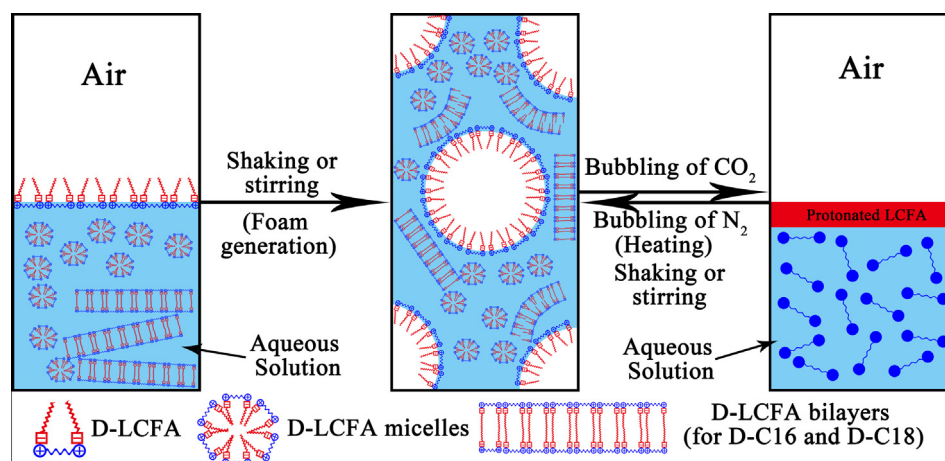


**Fig. 7.** Proposed mechanism of foaming and defoaming of D-LCFA aqueous solution upon the alternate bubbling of CO<sub>2</sub> and N<sub>2</sub>.

to be able to stabilize CO<sub>2</sub>-responsive aqueous foams. Considering both low-toxic and low-cost building blocks (LCFA and D 230), and simple preparation by Brønsted acid-base reaction, D-LCFA can be regarded as eco-friendly responsive surfactants. D-LCFA shows good surface activity and ability of generating stable aqueous foams. Increasing the chain length of D-LCFA was found to decrease foamability and increase foam stability, which was ascribed to the formation of bilayers. Bubbling of CO<sub>2</sub> into the foams stabilized by D-LCFA led to effective defoaming, while removal of CO<sub>2</sub> by bubbling of N<sub>2</sub> enabled re-generation of stable foams. This process is efficient and reversible. CO<sub>2</sub>-responsive aqueous foams stabilized by D-LCFA can be applied in situations where rapid foaming and defoaming is required, such as foam fracturing, foam enhanced oil recovery or recovering radioactive materials.

More interestingly, properties of D-LCFA can be tuned via changing spacers or tails. For example, varying number of EO or PO groups at polyetheramine spacer, or degree of unsaturation, chain length and linking groups of LCFA tails, can all change phase behavior of D-LCFA, which further determine the properties of foam or emulsion stabilized by D-LCFA. The external stimuli to control the foam stability can also be replaced by temperature (for EO and PO at spacer), PAG (photoacid generator) or salts. Maybe multiple responsive foam or emulsion can be stabilized by D-LCFA.

#### Acknowledgement

This work is supported by Natural Science Foundation of China (NSFC, 2133300).

#### Appendix A. Supplementary material

Supplementary data to this article can be found online at <https://doi.org/10.1016/j.jcis.2018.10.040>.

#### References

- [1] I. Cantat, S. Cohen-Addad, F. Elias, F. Graner, R. Höhler, O. Pitois, F. Rouyer, A. Saint-Jalmes, *Foams: Structure and Dynamics*, OUP Oxford, 2013.
- [2] J.F. Sadoc, N. Rivier, *Foams and Emulsions*, Springer Science & Business Media, 2013.
- [3] R. Pugh, *Adv. Colloid Interface Sci.* 64 (1996) 67.
- [4] F. Carn, H. Saadaoui, P. Massé, S. Ravaine, B. Julian-Lopez, C. Sanchez, H. Deleuze, D.R. Talham, R. Backov, *Langmuir* 22 (2006) 5469.
- [5] A.L. Fameau, A. Carl, A. Saint-Jalmes, R. von Klitzing, *ChemPhysChem* 16 (2015) 66.
- [6] A.L. Fameau, A. Saint-Jalmes, F. Cousin, B. Houinsou Houssou, B. Novales, L. Navailles, F. Nallet, C. Gaillard, F. Boué, J.P. Douliez, *Angew. Chem. Int. Ed.* 50 (2011) 8264.
- [7] B.P. Binks, R. Murakami, S.P. Armes, S. Fujii, A. Schmid, *Langmuir* 23 (2007) 8691.
- [8] S. Fujii, M. Suzuki, S.P. Armes, D. Dupin, S. Hamasaki, K. Aono, Y. Nakamura, *Langmuir* 27 (2011) 8067.
- [9] X. Yu, Z. Wang, Y. Jiang, F. Shi, X. Zhang, *Adv. Mater.* 17 (2005) 1289.
- [10] F.D. Jochum, P. Theato, *Chem. Soc. Rev.* 42 (2013) 7468.
- [11] A.L. Fameau, S. Lam, O.D. Velev, *Chem. Sci.* 4 (2013) 3874.
- [12] B.P. Binks, R. Murakami, S.P. Armes, S. Fujii, *Angew. Chem.* 117 (2005) 4873.
- [13] E. Chevallier, C. Monteux, F. Lequeux, C. Tribet, *Langmuir* 28 (2012) 2308.
- [14] L. Lei, D. Xie, B. Song, J. Jiang, X. Pei, Z. Cui, *Langmuir* 33 (2017) 7908.
- [15] M. Schnurbus, L. Stricker, B.J. Ravoo, B. Braunschweig, *Langmuir* 34 (2018) 6028.
- [16] S. Lam, E. Blanco, S.K. Smoukov, K.P. Velikov, O.D. Velev, *J. Am. Chem. Soc.* 133 (2011) 13856.
- [17] Y. Zhang, Y. Feng, Y. Wang, X. Li, *Langmuir* 29 (2013) 4187.
- [18] Y. Liu, P.G. Jessop, M. Cunningham, C.A. Eckert, C.L. Liotta, *Science* 313 (2006) 958.
- [19] P.G. Jessop, S.M. Mercer, D.J. Heldebrant, *Energy Environ. Sci.* 5 (2012) 7240.
- [20] Y. Zhang, H. Yin, Y. Feng, *Green Mater.* 2 (2014) 95.
- [21] X. Zhang, C. Wang, *Chem. Soc. Rev.* 40 (2011) 94.
- [22] Y. Li, H. Li, J. Chai, M. Chen, Q. Yang, J. Hao, *Langmuir* 31 (2015) 11209.
- [23] N. Sun, L. Shi, F. Lu, S. Xie, L. Zheng, *Soft Matter* 10 (2014) 5463.
- [24] G. Libralato, A. Volpi Ghirardini, F. Avezzi, J. Hazard, *Mater.* 176 (2010) 535.
- [25] M. Emo, M.J. Stébé, J.L. Blin, A. Pasc, *Soft Matter* 9 (2013) 2760.
- [26] N. Canilho, A. Pasc, M. Emo, M.J. Stébé, J.L. Blin, *Soft Matter* 9 (2013) 10832.
- [27] L. Wang, S. Liu, T. Wang, D. Sun, *Colloids Surf. A: Physicochem. Eng. Aspects* 381 (2011) 41.
- [28] C. Zhao, K. Tong, J. Tan, Q. Liu, T. Wu, D. Sun, *Colloids Surf. A: Physicochem. Eng. Aspects* 457 (2014) 8.
- [29] P. Xu, Z. Wang, Z. Xu, J. Hao, D. Sun, *J. Colloid Interface Sci.* 480 (2016) 198.
- [30] X. Chen, X. Ma, C. Yan, D. Sun, T. Yeung, Z. Xu, *J. Colloid Interface Sci.* 534 (2018) 595.
- [31] Y. Zhu, J. Jiang, Z. Cui, B.P. Binks, *Soft Matter* 10 (2014) 9739.
- [32] P.D. Pudney, K.J. Mutch, S. Zhu, *Phys. Chem. Chem. Phys.: PCCP* 11 (2009) 5010.
- [33] F.M. Menger, J.S. Keiper, *Angew. Chem. Int. Ed.* 39 (2000) 1906.
- [34] M.J. Rosen, D.J. Tracy, *J. Surfactants Deterg.* 1 (1998) 547.
- [35] A. Campbell, G. Lakshminarayanan, *Can. J. Chem.* 43 (1965) 1729.
- [36] M.S. Akhter, *Colloids Surf. A: Physicochem. Eng. Aspects* 121 (1997) 103.
- [37] Z. Briceño-Ahumada, A. Maldonado, M. Imperor-Clerc, D. Langevin, *Soft Matter* 12 (2016) 1459.
- [38] B.P. Binks, S. Campbell, S. Mashinchi, M.P. Piatko, *Langmuir* 31 (2015) 2967.
- [39] S.A. Shkulipa, W. Den Otter, W. Briels, *Biophys. J.* 89 (2005) 823.
- [40] W. Richtering, *Curr. Opin. Colloid Interface Sci.* 6 (2001) 446.
- [41] W. Xu, H. Gu, X. Zhu, Y. Zhong, L. Jiang, M. Xu, A. Song, J. Hao, *Langmuir* 31 (2015) 5758.
- [42] Z. Chu, Y. Feng, *Chem. Commun.* 46 (2010) 9028.
- [43] F. Menger, C. Littau, *J. Am. Chem. Soc.* 115 (1993) 10083.
- [44] R. Nagarajan, *Langmuir* 18 (2002) 31.
- [45] J. Du, R.K. O'Reilly, *Soft Matter* 5 (2009) 3544.
- [46] A.L. Fameau, A. Arnould, A. Saint-Jalmes, *Curr. Opin. Colloid Interface Sci.* 19 (2014) 471.
- [47] D. Varade, D. Carriere, L.R. Arriaga, A.L. Fameau, E. Rio, D. Langevin, W. Drenckhan, *Soft Matter* 7 (2011) 6557.
- [48] E. Rio, W. Drenckhan, A. Salonen, D. Langevin, *Adv. Colloid Interface Sci.* 205 (2014) 74.
- [49] A.L. Fameau, T. Zemb, *Adv. Colloid Interface Sci.* 207 (2014) 43.
- [50] J. Kanicky, A. Poniatowski, N. Mehta, D. Shah, *Langmuir* 16 (2000) 172.
- [51] C. Liang, J.R. Harjani, T. Robert, E. Rogel, D. Kuehne, C. Ovalles, V. Sampath, P.G. Jessop, *Energy Fuels* 26 (2012) 488.
- [52] D. Li, B. Ren, L. Zhang, J. Ezekiel, S. Ren, Y. Feng, *Chem. Eng. Res. Des.* 102 (2015) 234.
- [53] J. Wang, M. Liang, Q. Tian, Y. Feng, H. Yin, G. Lu, *J. Colloid Interface Sci.* 523 (2018) 65.
- [54] G. Ren, L. Wang, Q. Chen, Z. Xu, J. Xu, D. Sun, *Langmuir* 33 (2017) 3040.
- [55] P. Anastas, N. Eghbali, *Chem. Soc. Rev.* 39 (2010) 301.
- [56] Y. Feng, Z. Chu, *Soft Matter* 11 (2015) 4614.